CHALMERS
UNIVERSITY OF TECHNOLOGY

Parameter sensitivity of a wood chips flow model

Citation for the original published paper (version of record):

Evysdotter, S., Vikström, T., Rasmuson, A. (2025). Parameter sensitivity of a wood chips flow model. Canadian Journal of Chemical Engineering, 103(2): 868-879.
http://dx.doi.org/10.1002/cjce.25435

Received: 12 December 2023 | Revised: 31 May 2024 | Accepted: 10 June 2024

DOI: 10.1002/cjce.25435

RESEARCH ARTICLE

THE CANADIAN JOURNAL OF CHEMICAL ENGINEERING

Parameter sensitivity of a wood chips flow model

Sofia Evysdotter[1] | **Tomas Vikström**[1,2] | **Anders Rasmuson**[3]

[1]Valmet AB, Sundsvall, Sweden

[2]Department of Fibre and Polymer Technology, Royal Institute of Technology, Stockholm, Sweden

[3]Department of Chemistry and Chemical engineering, Chalmers University of technology, Gothenburg, Sweden

Correspondence
Tomas Vikström, Valmet AB, Sundsvall, Sweden.
Email: tomas.vikstrom@valmet.com

Present address
Tomas Vikström, Valmet, Gustaf Gidlöfs väg 4, 85194, Sundsvall, Sweden.

Funding information
Energimyndigheten, Grant/Award Number: 45123-1

Abstract

A computational fluid dynamics (CFD) study of the parameter sensitivity of a wood chips model was performed on an industrial impregnation vessel, which is the first step in a continuous cooking system. The solid and liquid phases were both treated as continua and it was found that the continuum model for the solid wood chips phase could capture the previously observed oscillating formation of arches in the contracting part of the vessel, which will occur at different levels of volume fraction depending on the material constants. The parameters that were examined are the solid pressure, permeability, viscosity, and wall friction. It was found that all the parameters strongly affect the distribution of the wood chips in the vessel as well as the oscillation effects, hence also the flow field which is important to accurately predict in order to ensure optimal performance of the impregnation vessel. Thus, correct material data for these types of simulations are crucial to the outcome and should be chosen for the appropriate situation and bio-material.

KEYWORDS

arching, CFD, multiphase, numerical model, wood chips

1 | INTRODUCTION

Fibrous material pulp can be produced either chemically, mechanically, or via a combination of both, using a lignocellulosic raw material such as wood or straw. Wood is mainly made up of cellulose, hemicellulose, and lignin, all which are large polymers. To separate the fibres in order to make pulp, the lignin, which provides compressive strength and waterproofing of the cell walls, must be dissolved. The process of removing lignin in chemical wood pulping starts with pre-steaming of the wood chips followed by impregnation of cooking liquor, and next the addition of heat. The chemical delignification process is carried out in either batch or continuous digester vessels with sodium hydroxide and sodium sulphide as cooking chemicals, according to Kassberg.[1] Kraft pulping is a highly complex process where the hydrodynamics of a multi-component multi-phase flow interact with the chemical kinetics, reactions, and thermodynamics in a large vessel. In order to fully comprehend the conditions prevailing in the cooking equipment, the mass, heat, and momentum transport in three dimensions must be considered. The continuous pulp digester shows some similarities with a packed bed of solids in which a fluid is passing, in the sense that the way the solids are packed in the vessel affects how the liquid is distributed. Even though the chips are also moving, they do not move around freely in the liquid phase but are continuously in contact with each other when the volume fraction exceeds a critical value, as is the situation in cooking equipment for pulp. The way the solids are packed depends on their deformation and orientation, which affect the distribution of the liquid, which will again affect the distribution of the solids.

A cooking system can consist of two vessels, including a separate vessel for impregnation and a digester; in such a system, wood chips and an alkaline solution are fed into the impregnation vessel giving sufficient residence time and allowing the cooking chemicals to diffuse into the active sites of reaction in the wood chips prior to entering the digester, as per Kassberg.[1] An even distribution of the liquor in the impregnation vessel is important to ensure that the cooking chemicals are evenly distributed in the wood chips when entering the digester, where heat is added to start the delignification reactions. In the impregnation vessel, the delignification reactions are limited since the temperature is kept, in the context, rather low. The mechanical properties of the wood chips will thus remain constant.

An important parameter when modelling pulp digesters is the kappa number, a measure of the amount of lignin in the pulp. Predicting the kappa number predicts the performance of the digester, and to do so requires a good understanding of both the hydrodynamic conditions prevailing in the reactor, as well as the heat and mass transfer. The packing of the bed has a significant effect on the permeability distribution, thus a well predicted flow field is essential to predict the kappa number and operation of the cooking equipment. This requires a model for the solid interactions and the most used model for wood chips is the one proposed by Härkönen,[2] who developed a model of the solid pressure as a function of the kappa number and volume fraction and for the flow resistance as a function of volume fraction. The models by Härkönen were developed under the assumption that there is rotational symmetry, no shear forces, and that the solid pressure and flow resistance are isotropic. These assumptions result in no friction between the walls of the vessel and the chip bed. Several authors have used this model for describing the solid interactions in their digester models, including Michelsen and Foss,[3] Wiesnewski et al.,[4] Bhartiya et al.,[5] Fan,[6] Kayihan et al.,[7] Pougatch et al.,[8] Rantanen,[9] and Laakso et al.[10]

The inter-phase flow resistance of the chip bed is modelled by Härkönen using a modified Ergun equation. The constants in this modified equation have been under investigation by several authors. In 2002, Lee[11] conducted experiments on a laboratory scale column of packed wood chips. The pressure drop was measured against superficial velocity, kappa number, void fraction, and compacting pressure, and it was concluded that Härkönen's constants in the equation for the pressure drop are too low. Also, the constants should not be universal constants since the shape and size of the solids in the bed greatly affect the pressure drop. Uncooked chips do not have the same pressure drop as cooked chips, since the pressure drop is largely dependent on the void fraction of the bed which in turn is dependent on the kappa number. The void fraction is not evenly distributed over the column and correlations based on the average void fraction is likely insufficient in predicting the pressure drop. Alaqqad et al.[12] present a list of constants for various chip sizes and materials from previous investigations of the constants in the drag model.[12] The pressure drop in porous media for low Reynolds numbers can be estimated using the Darcy equation. Zeng and Grigg[13] defined a criterion to determine when deviation from Darcy flow occurs and recommend a critical Forchheimer number of 0.11. Ghane et al.[14] measured in-situ the coefficients for the Forchhiemer number for bio reactors where wood chips are packed to some extent and concluded that the Forchheimer equation predicts the flow rate better than the Darcy equation.

Pougatch et al.[8] developed an axisymmetrical model where the chip bed is modelled as a Bingham fluid in which the threshold shear stress is a linear function of the solid pressure. The interaction with the wall is also a function of the solid pressure. The particle interaction is modelled in a similar way as the wall–particle friction; however, it is assumed that the particles move more easily against the rather smooth wall than against each other. Fan[6] examined the effect of particle size on chips compressibility using CFD in an industrial digester; the computational domain was simplified to not include the complex bottom part. It was found that the compressibility of the chips significantly affects the cooking performance due to the effect on the residence time.

Vessels used for pulping are geometrically similar to silos for storage of agricultural material and hence experience some of the same phenomena. In silos, as in a pulp digester, the material is granular and the discharge is in the bottom; however, one important difference is that there is no liquid in silos but air instead, which greatly affects the drag force between the components, due to the difference of several orders of magnitude in the density between the applications. This results in small velocity changes in the liquid case which result in larger changes in drag force at the same velocity. Since large forces are transmitted to the solid phase even at small changes, the packing of the solid phase will increase more. The same is true for the opposite effect if the liquid is moving counter current to the solid phase: the packing will be loosened up to a greater extent. A common situation occurring in silos is the formation of an arch adjacent to the outlet. Drescher et al.[15] refer to *arching* as:

> the spontaneous formation of an arch-like supported stagnant mass of bulk material in a bin or hopper upon opening of the outlet or during gravitational flow.

Further, it is stated that the formation of arches depends on the geometry and the ratio of the outlet size to the vessel size. Other factors that affect the tendency to form arches are examined by Hinterreiter et al.,[16] who concluded that, for wood chips, the shape, size, and aspect ratio are highly important in understanding the arching phenomena. Yoshida[17] found, using discrete element modelling (DEM), that the periodicity of the pulsation of the particles in the upper part of the silo is identical to the variations in pressure on the silo walls, which long have been thought of as a result of the formation and collapse of arches. In 2001, To et al.[18] examined the probability of jamming due to convex arch formation in 2D-silos. Arches that form at a bottleneck are a large problem when clogging or jamming occurs. As for architectural arches, these can hold up the load of the material above, which Hidalgo et al.[19] analyzed using DEM.

The prevailing view in digester modelling is that the hydrodynamic plays a very important role in predicting the performance of the digester, hence the packing degree of the digester cannot be predefined. This article is focused on the hydrodynamic conditions and the parameters that affect the distribution of chips and liquor. A sensitivity analysis on these model parameters will be performed and presented. As previously mentioned, it is highly important to predict the interaction between the chips and liquor correctly, as is the interaction between the chips themselves, as well as with the wall, which are functions of the volume fraction and solid pressure. Thus, getting the solid pressure model right will greatly affect the outcome of the simulations. The solid pressure corresponds to the deformability of the chips column, which includes compression and orientation. Various sorts of wood have different properties and it can thus be assumed that a packed column of various chips, with varying size and temperature and also varying moisture content will not be distributed in the column in the same way. The solid pressure and the deformability of the chips column can be viewed as a measure of how the wood chips can be oriented due to an applied force. Removing the force will nevertheless not result in a random distribution of the chips again, thus there is a hysteresis effect when the chips column is subjected to a load and then again unloaded. Varying constants in the constitutive equation for the solid pressure can be regarded as varying the stiffness of the chips column. However, since the solid pressure is included in several other properties, altering the constants in the function for the solid pressure will not be sufficient to isolate which properties are of most significance. As a base case which will be the origin of all variations of this sensitivity analysis are the models and parameter values presented by Härkönen[2] and further extended by Pougatch et al.[8] The values of the parameters are presented in Section 5.

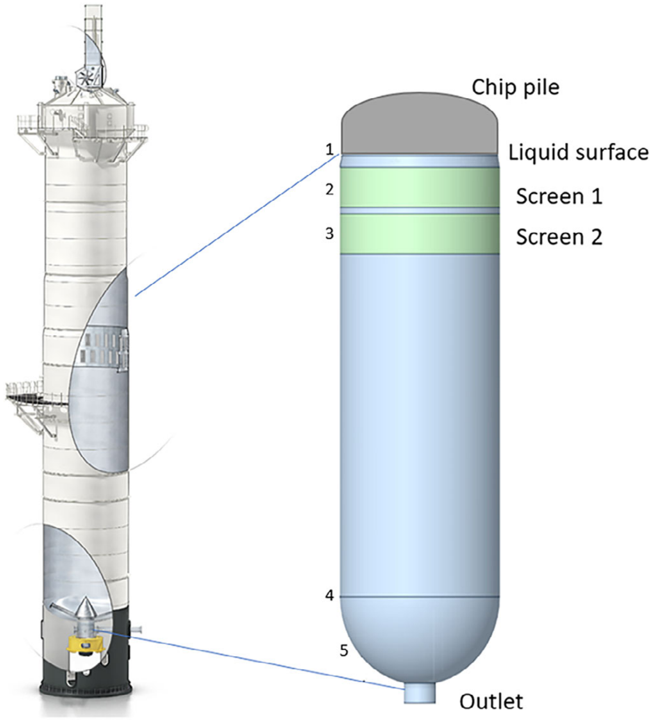

FIGURE 1 The impregnation vessel; diameter = 8.8 m, height = 46 m, liquid level = 24 m above spherical part, outlet diameter = 1.75 m. Left side, a 3D-rendering of the complete impregnation vessel. Right side, the computational domain, 360 degrees.

2 | AIM OF THIS WORK

The aim of this work is to investigate the Eulerian multiphase flow models initially developed by Härkönen and further extended by Pougatch et al. in order to determine the sensitivity of the output depending on the most significant model constants and to illustrate the importance of choosing the correct constants depending on the properties of the actual material. This article will therefore be limited to the impregnation vessel and resolving the hydrodynamics where the effect of the processes on the particle properties are limited. The hydrodynamic conditions are analogous in the digester, hence the Eulerian model can later be further extended to include the chemical reactions and mass transfer that describes the complete delignification process. This is one reason for the utilization of CFD, as compared to DEM, as well as the size of the equipment and, hence, number of particles in the system, which is in the order of billions.

3 | SET UP

In a two-vessel continuous cooking system, the impregnation vessel precedes the digester and is utilized to impregnate the wood chips with cooking liquor. First, steam is added to remove the air in the chips; second, the cooking liquor is added but the temperature remains rather low, keeping the reaction rate slow. The vessel includes two screen packages, see Figure 1 at positions 2 and 3, where liquid is extracted and two vertical positions of injection points, Figure 1, positions 4 and 5; the chips are fed into the vessel in the top and 2 m above the screens is the liquid level, position 1, hence the impregnation vessel is not completely filled with liquid. The cooking liquid is fed into the vessel at the top and also at the two injection positions, which are placed around the spherical part of the bottom for the current geometry, to dilute the outflow. The upper injection point is located at the intersection of the spherical bottom and cylindrical upper part. The lower injection point is located at a radius of 3.2 [m].

4 | GOVERNING EQUATIONS

In order to model this multiphase system with dense particle loading, the Euler–Euler method was chosen; due to the number of particles, the Lagrangian approach is not applicable. The focus of this work is on the hydrodynamic conditions, however it is desirable to extend the model to include mass and heat transport, which excludes DEM models at the moment. The Euler–Euler method treats all included phases as interpenetrating continua. The following equations constitute the inhomogeneous model that has been used in this work.

$$\frac{\partial}{\partial t}(\varepsilon_\alpha \rho_\alpha) + \nabla \cdot (\varepsilon_\alpha \rho_\alpha \mathbf{U}_\alpha) = \mathbf{S}_{\mathrm{MS}_\alpha} + \sum_{\beta=1}^{N_p} \Gamma_{\alpha\beta} \tag{1}$$

In Equation (1), the continuity equation, the first term on the left side is accumulation, and the second term is the convective transport where $\mathbf{U}_\alpha$ is vector velocity. On the right-hand side, the first term denotes the user specified mass sources and the second term is the mass flow rate per unit volume from phase β to α.

$$\frac{\partial}{\partial t}(\varepsilon_\alpha \rho_\alpha \mathbf{U}_\alpha) + \nabla \cdot (\varepsilon_\alpha (\rho_\alpha \mathbf{U}_\alpha \otimes \mathbf{U}_\alpha)) = -\varepsilon_\alpha \nabla p_\alpha + \nabla \cdot \left(\varepsilon_\alpha \mu_\alpha \left(\nabla \mathbf{U}_\alpha + (\nabla \mathbf{U}_\alpha)^T\right)\right) + \mathbf{S}_{\mathrm{M}\alpha} + \mathbf{M}_\alpha \tag{2}$$

In the momentum Equation (2), the terms on the left hand side are accumulation and convection, respectively. The first term on the right-hand side is the pressure gradient and the second term describes the transport due to viscous forces. $\mathbf{S}_{\mathrm{M}\alpha}$ is the source term taking into account the external body forces and user defined momentum sources. The forces acting on phase α due to presence of other phases is included in the term $\mathbf{M}_\alpha$. This will be explained in more detail below.

To close the equation system, two constraints are needed. The first one is that the volume fractions sum to unity.

$$\sum_{\alpha=1}^{N_p} \varepsilon_\alpha = 1 \tag{3}$$

The second constraint is that all phases share the same pressure field.

$$p_\alpha = p \;\; \forall \; \alpha = 1, \ldots, N_{\mathrm{p}} \tag{4}$$

4.1 | Momentum transfer

When more than one phase is present and the flow is considered in-homogeneous, the inter-phase momentum transfer occurs because of inter facial forces acting on each phase α due to interaction with phase β. The inter facial forces are equal, opposite, sum to zero, and arise from independent physical phenomena such as drag force, solid particle collisions, and so forth.

4.1.1 | Drag force

The interphase drag force is generally expressed as follows:

$$\mathbf{M}_\alpha = c_{\alpha\beta}^{(d)} \left(\mathbf{U}_\beta - \mathbf{U}_\alpha\right) \tag{5}$$

in Equation (2). In the multiphase model utilized in this work, the drag coefficient is defined as follows:

$$\mathbf{D}_{\alpha\beta} = C_D \rho_\alpha A \left| \mathbf{U}_\beta - \mathbf{U}_\alpha \right| \left(\mathbf{U}_\beta - \mathbf{U}_\alpha\right) \tag{6}$$

where $\mathbf{D}_{\alpha\beta}$ is the total drag on phase β from phase α and A is the projected area of the body in the flow direction according to Ansys.[20] The total drag for this application is defined as follows:

$$\mathbf{D}_{\alpha\beta} = \frac{\varepsilon_\beta}{\varepsilon_\alpha} \left(R_1 \frac{\varepsilon_\beta}{\varepsilon_\alpha} + R_2 \left| U_\beta - U_\alpha \right| \right) \tag{7}$$

where the constants R_1 and R_2 will be described in Section 4.4.

4.1.2 | Particle collision model

The interaction between the solid particles present is modelled via the solid pressure. The model used is the one developed by Härkönen[2] which relates the solid pressure to a volume fraction.

$$\varepsilon_\beta = k_0 + P_s^{k_1}(k_2 + k_3 \ln(\kappa)) \tag{8}$$

which, with some algebra, can be arranged as follows:

$$P_s = P_{s0}\left(\frac{\varepsilon_\beta - \varepsilon_0}{\ln(\alpha/\kappa)}\right)^{1/d} \tag{9}$$

where κ is the kappa number which describes the degree of delignification and P_{S0} which is a material constant that is related to the elasticity of the chips column. ε_0 is the material constant which describes the critical point of volume fraction where enough solids are present to form a network according to de Kretser et al.,[21] and α and d are model constants.

4.2 | Viscosity

The viscosity, which is a measure of the inter-particle friction, is treated as a Bingham fluid, which implies that there is a threshold value of the force needed to disrupt the network of solids, as first implemented by Pougatch et al.[8] This is reasonable since one of the most significant characteristics of this matter of solid particles is the yield stress. On the macro level, a large number of particles will behave as a solid until the yield stress is exceeded; beyond that point, the particles will move as a highly viscous fluid.

$$\mu_{\text{eff}} = \mu + \frac{\tau_0}{\gamma} \tag{10}$$

where $\tau_0 = f(P_S)$ and γ is the shear strain rate.

4.3 | Wall friction

The solid phase fluid interaction with the wall is analogous to the behaviour of two non-deforming solids in contact. The solid phase fluid remains in rest until an applied stress exceeds the frictional stress between the wall and the solid phase. Above this critical stress, the solid phase fluids moves along the wall. Pougatch et al.[8] used a model for the solids behaviour at the wall, in which it is possible for the solid phase to slip at the wall. The tangential yield stress is proportional to the solid pressure P_S. The interaction between the wall and the solids are similar to the behaviour between the solids themselves. Pougatch et al. reason that it is fair to assume that the chips in the digester slip more easily against the digester walls than against each other, based on the surface roughness. After movement is initiated by exceeding the critical stress, the tangential stress at the wall is a function of the solid pressure P_S. The velocity at the wall is not resolved but modelled as a partial slip condition which transfers only the momentum into the fluid body.

$$\tau_{\text{wall}} = f_{\text{wall}} P_s \tag{11}$$

where f_{wall} is the friction coefficient.

4.4 | Permeability model

The modified Ergun equation presented by Härkönen[2] is as follows:

$$\frac{\Delta P}{\Delta l} = R_1 \frac{(1-\varepsilon_2)^2}{\varepsilon_2^3} v + R_2 \frac{(1-\varepsilon_2)}{\varepsilon_2^3} v^2, \tag{12}$$

where the first term is the laminar term and describes the flow resistance due to viscous forces, the second term is flow resistance for 'turbulent' flow, ε_2 is the void fraction, and R_1 and R_2 are model constants.

4.5 | Boundary conditions

The computational domain is a 2D axisymmetrical representation of an existing impregnation vessel utilized at a mill. The domain is limited to the liquid level of the equipment, where a pressure boundary condition describes the conditions in the top of the impregnation vessel. The outlet condition is a volumetric flow which is determined by the pump to the digester in the mill. There are also two screen packages in the top which extract liquid, and two positions in the lower part of the vessel where liquid is injected; both screens and injections are modelled as source terms. The flow rates are specified in Table 1, and the geometry can be seen in Figure 1 with boundaries marked and additionally described in Section 3.

4.6 | Numerical CFD

The numerical simulations executed with ANSYS CFX 2022R1 are transient, with timestep $t = 0.001$ s and solved with the high resolution numerical scheme. The mesh consists of $3 \cdot 10^4$ polyhedral cells with an average size of 0.2 m. Both phases are treated as continua, hence the

TABLE 1 Boundary conditions.

Boundary	Value	Units
Inlet	0	[Pa]
Outlet	0.5	[m^3/s]
Screen	0.025	[m^3/s]
Dilution	0.1	[m^3/s]

TABLE 2 Model constants of base case from Härkönen[2] and Pougatch et al.[8]

Constant	Value	Units
P_{s0}	$2.83 \cdot 10^5$	Pa
α	395	–
κ	150	–
d	0.59	–
R_1	$4.6 \cdot 10^3$	kg/m^3s
R_2	$3.9 \cdot 10^6$	kg/m^3s
f_{Wall}	0.25	–

particles are not resolved, and the particle size is $d_p = 0.01\,\mathrm{m}$. A finer mesh with half the cell size have been tested for one set of parameters, to ensure grid independence. The pressure field shows no significant deviation dependent on cell size. The choice of the time step is to ensure numerical stability caused by rapid and large force derivatives on one side, on the other is minimizing computational time. A smaller timestep of 0.0001 s have been tested which results in same overall behaviour.

5 | SENSITIVITY ANALYSIS OF MODELS FOR CHIPS FLOW

As the base case, the model and constants presented by Härkönen and further developed by Pougatch et al., is used. The model constants for Equations (9), (11), and (12) used are presented in Table 2 and the variations for the sensitivity analysis are presented in Table 3. Each parameter is changed one at the time and has been chosen to provide a significant deviation from the original values, but still be reasonable and numerically stable. The results from each test is presented in Sections 5.1–5.4.

In the current geometry an arch is formed between the walls of the vessel and the internal conical structure. The arch is built up and debilitated to be rebuilt again, periodically, as shown in Figure 2. As the arch forms the pressure below it is lowered due to the outlet condition,

TABLE 3 Model constants for sensitivity anlysis.

Constant	Low value	High value
P_{s0}	$1 \cdot 10^5$	$8 \cdot 10^5$
R_1	$0.25 \times (4.6 \cdot 10^3)$	$4 \times (4.6 \cdot 10^3)$
R_2	$0.25 \times (3.9 \cdot 10^6)$	$4 \times (3.9 \cdot 10^6)$
f_{Wall}	0.125	0.4

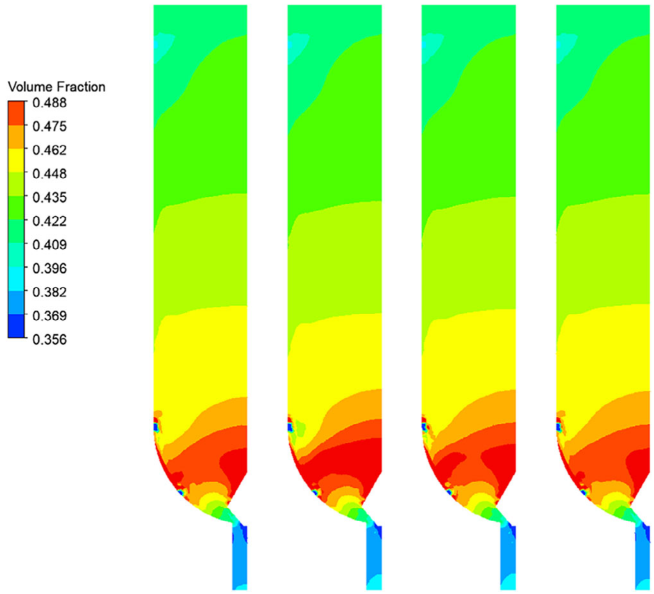

FIGURE 2 Base case at four consecutive times, volume fraction of chips. Arch formation and tear down.

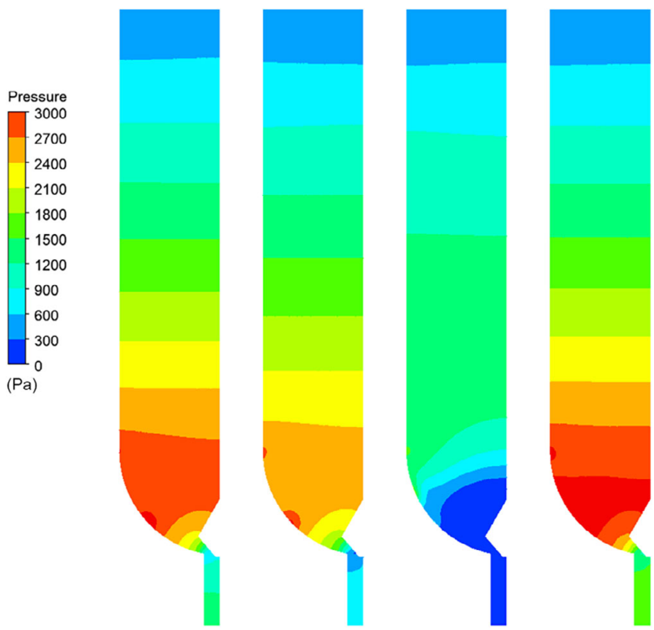

FIGURE 3 Base case at four consecutive times, pressure during arch formation and tear down.

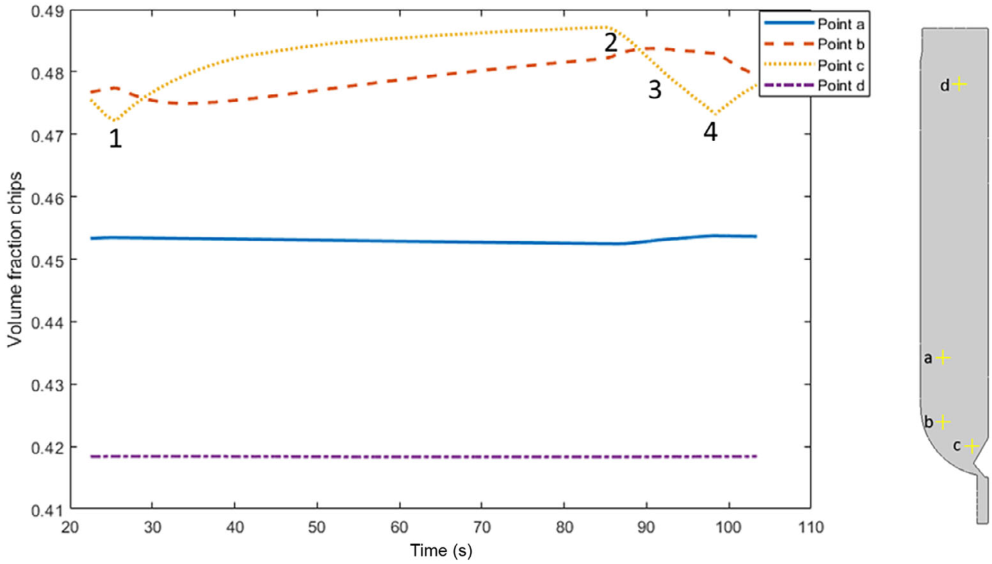

FIGURE 4 Average volume fraction during arch formation and collapse. 1-no arch, 2-full arch, 3-arch collapse, 4-no arch, same as 1. Monitor points a–d marked in geometry.

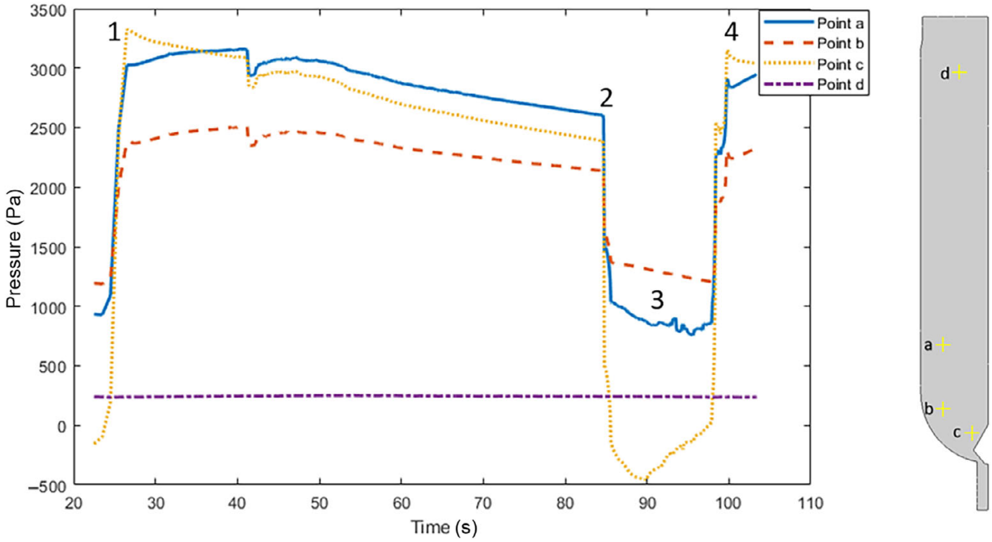

FIGURE 5 Average pressure during arch formation and collapse. 1-no arch, 2-full arch, 3-arch collapse, 4-no arch, same as 1, corresponding to Figure 4. Monitor points a–d marked in geometry.

at a certain point it breaks, and the pressure rises, as shown in Figure 3. The arch is formed as the material is flowing downwards due to gravity and the pump down streams the vessel, which is modelled by a boundary condition of constant outlet velocity. The periodic formation and breakage of the arch can be seen during the simulation when monitoring the volume fraction of chips, as shown in Figure 4. The corresponding pressure during the simulation at the same points in the domain can be seen in Figure 5, the periodicity is identical, in accordance with previous mentioned theory and DEM simulations by Yoshida.[17]

5.1 | Solid pressure

The function describing the solid pressure has been examined by varying the constant P_{S0}, the values of the base case and the variations can be found in Tables 2 and 3, respectively. As mentioned in the introduction, the solid pressure is included in the models describing the interaction of the chips with the vessel and the chips themselves, the viscosity. Lowering P_{S0} will lower the viscosity and the load of the chips column that the wall can carry. A high value of P_{S0} corresponds to a stiffer and less deformable type of chips. It can be seen in Figure 6 that with a higher P_{S0}, the column of chips is less packed, correspondingly a lower P_{S0} results in more packed column due to the fact that liquid flow would have a greater impact on the softer chips. The chips are then more packed by the same drag force, which results in the bridge formation at a higher value of volume fraction. It can also be noted that with the higher P_{S0}, the distribution of chips is more even, not only in the vertical flow direction, but also in the horizontal. Further, as can be

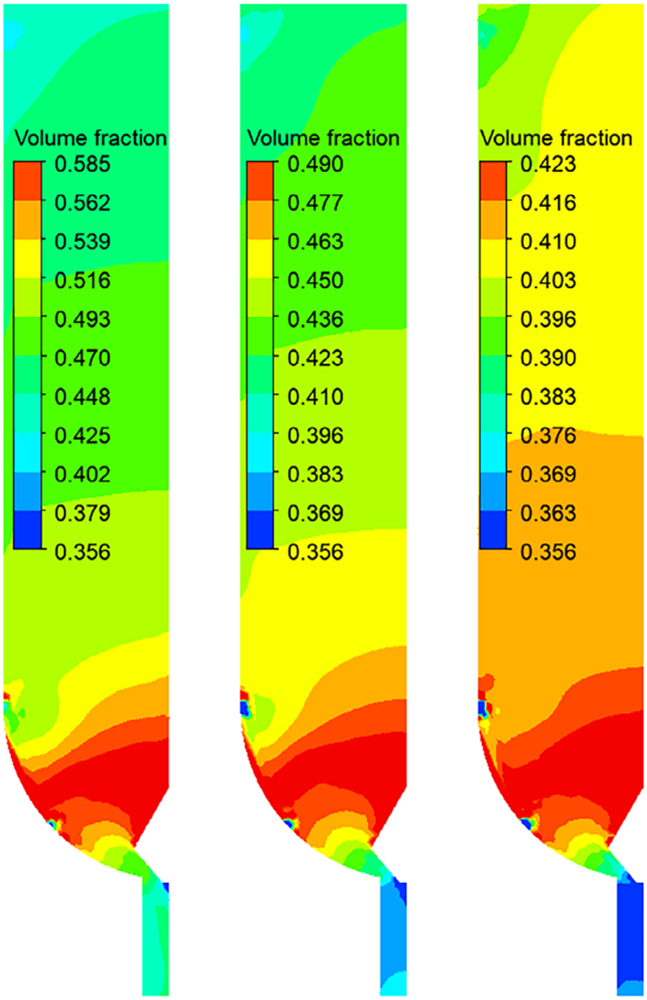

FIGURE 6 Volume fraction of chips for three different values of P_{S0}. $P_{S0} = 100{,}000$ Pa, $P_{S0} = 283{,}500$ Pa, $P_{S0} = 800{,}000$ Pa.

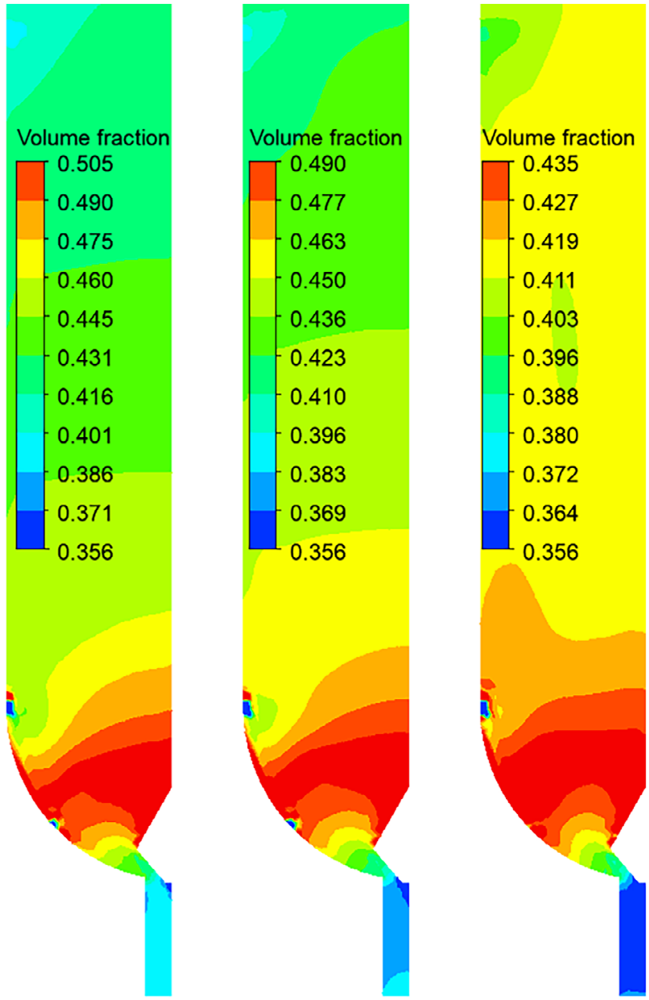

FIGURE 8 Volume fractions of chips for three different wall friction coefficients. From left: $f_W = 0.125$, $f_W = 0.25$, $f_W = 0.4$.

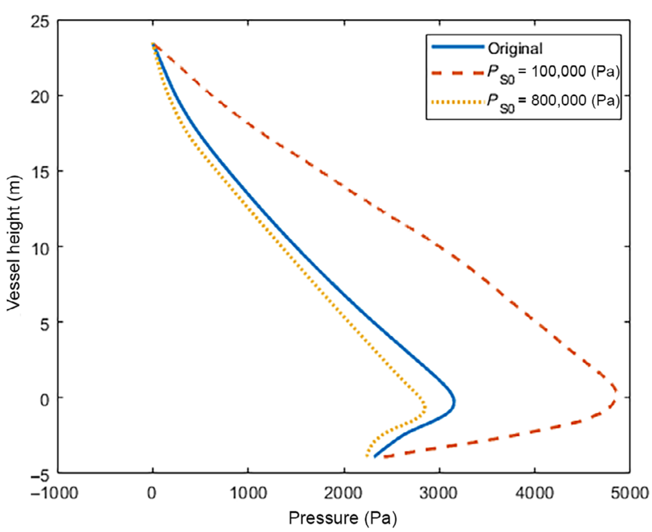

FIGURE 7 Pressure profile through reactor for three different values of P_{S0}.

seen in Figure 7, the pressure drop is lower for the higher P_{S0}, which is to be expected due to the lower volume fraction of the chips in the bottom of the vessel. The formation of arches is a matter of force balance; as long as the viscous forces are not exceeded by other forces, such as gravity or hydraulic pressure, there is a possibility for an arch to form and be sustained.

5.2 | Viscosity

Since the viscosity is a measure of the friction between the particles, it only exist when the particles are in contact with each other, which is when a critical volume fraction of particles is exceeded and hence the solid pressure will also exist. The viscosity of the solid phase is as mentioned, described with a Bingham model and is a function of the solid pressure and the shear strain rate, see Equation (10). Depending on the solid pressure, the viscosity will vary in the domain during the simulations. Varying P_{S0} will also vary the viscosity. As Pougatch et al.[8] in previous work have stated, a high constant viscosity is not adequate for modelling the wood chips phase; the non-Newtonian approach is necessary to achieve a sufficiently accurate solution of the velocity field.

5.3 | Wall friction coefficient

The model for the interaction with the wall, suggested by Pougatch et al., is utilized and the friction coefficient is set to three different values (low, base, and high) as presented in Tables 2 and 3. For the case with the lower coefficient, which corresponds to half the base case, but still in a reasonable range for the application, it is noted that the pattern of the packing of the chips is the same as for the base case; the actual level of volume fraction of chips is however higher, as seen in Figure 8. The highest value reached is in the formation of an arch between the reactor wall and the cone structure inside the vessel, for all cases. The higher level of packing can be explained by the fact that the wall carries less of the load of the column, which causes it to settle more. This is in line with the Janssen effect where some of the load of the particulate phase is carried by the walls, as per Mahajan et al.[22] The opposite is true for the higher wall friction coefficient, where the column of chips is less packed, due to the fact that now the wall carries more of the load of the chips, as shown in Figures 8 and 9.

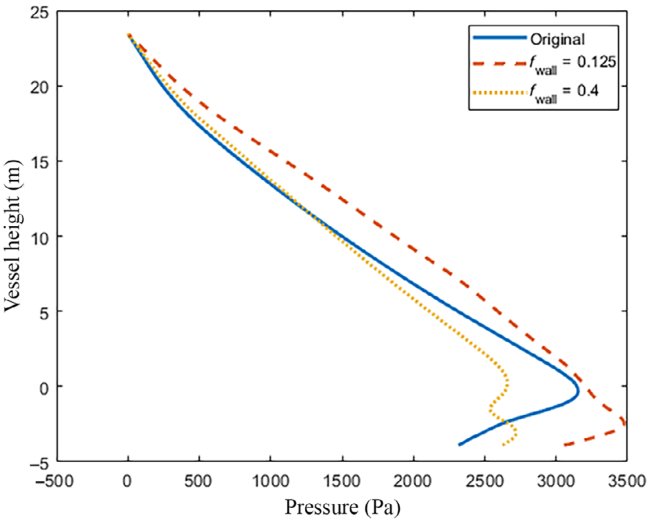

FIGURE 9 Pressure profile through reactor for three different wall friction coefficients.

5.4 | Permeability

To predict the pressure drop in vessels containing chips and liquor, the Ergun equation has previously been applied to model the permeability. A compilation of coefficients for different types of wood was presented by Alaqqad et al.[12] The negative values of the coefficient R_2 are not realistic; the pressure drop cannot decrease proportional to the square of the velocity. These negative coefficients can thus only be regarded as curve fitting. For the sensitivity analysis, the base case is the coefficients presented by Härkönen, and the high case is Härkönen's coefficients multiplied by four. This results is approximately the same

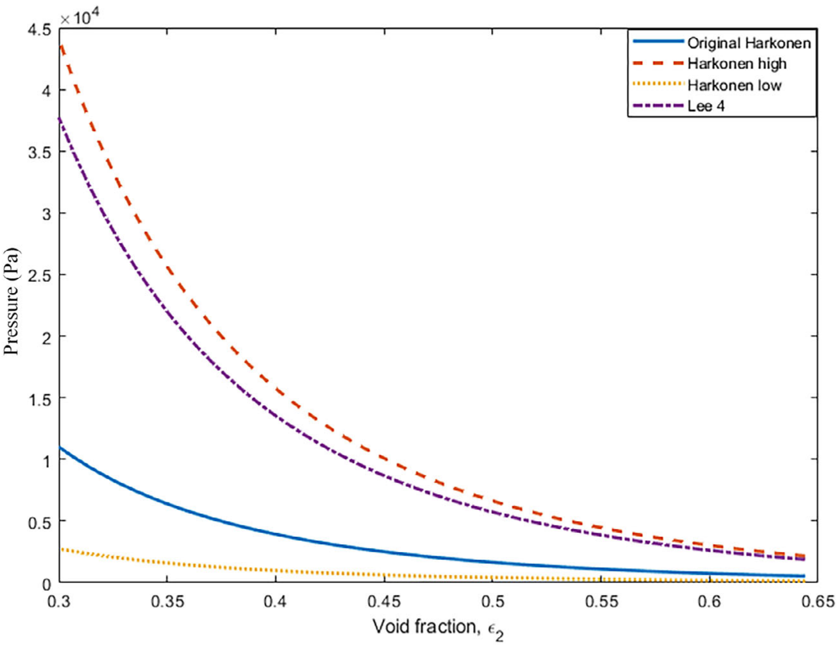

FIGURE 10 Expected pressure drop for fixed velocity of 0.01 [m/s] for values of R_1 and R_2 in Table 3. Lee for reference from Alaqqad et al.[12]

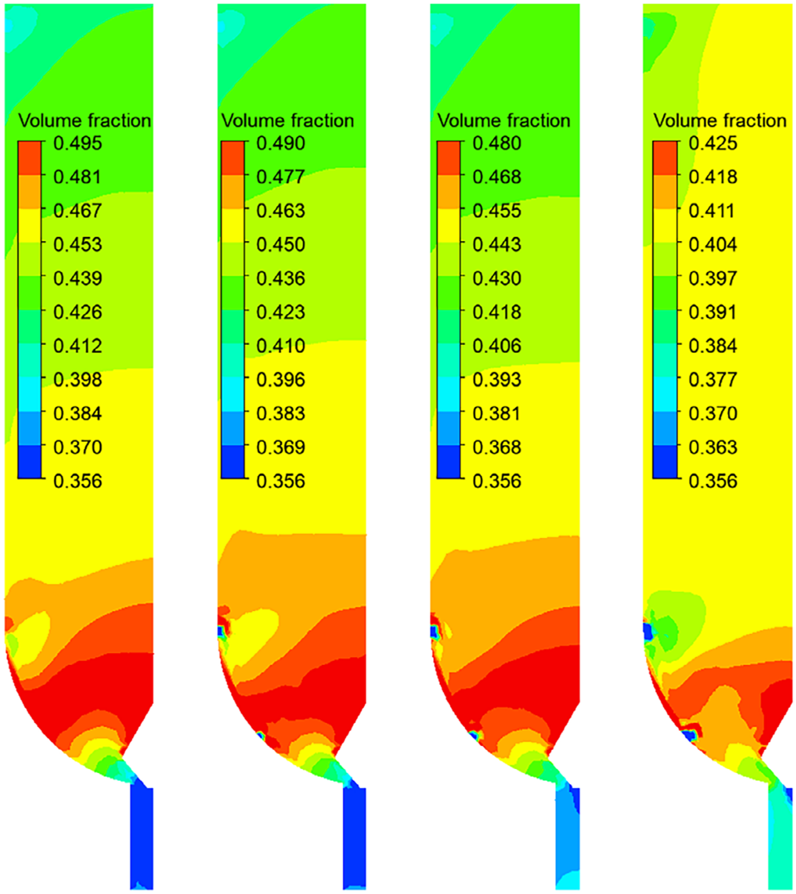

FIGURE 11 Degree of packing through reactor for various values of R_1 and R_2. From left: Low case, $R_2 = 0$, base case, high case.

pressure drop as for constants by Lee, presented by Alaqqad et al.,[12] see Figure 10. The coefficients by Härkönen have been criticized for being rather low; however, for the sake of the analysis, the lower-case coefficients are Härkönen's divided by four. To further test the sensitivity of the models, the value of R_2 is set to 0. As seen in Figure 11, the volume fraction of chips is dependent on the coefficients R_1 and R_2. The case with the lowest coefficients results in a higher volume fraction in the region where the arch is formed, letting $R_2 = 0$ results in approximately the same pattern and value. As expected, for the higher values of R_1 and R_2, the volume fraction of chips is lower than both the case with the low coefficients as well as the base case. However, all cases show periodical formation and breakage of an arch between the walls of the vessel and the conical structure in the middle. The pressure drop through the vessel for the various values of R_1 and R_2 can be seen in Figure 12. The pressure drop for the low case is almost identical to the case where $R_2 = 0$, where the later would represent a situation where the inertial forces would be negligible compared to viscous forces. Calculating the Forcheimer number according to Ghane et al.[14] gives $Fo = 5$ which results in a large deviation from Darcy flow according to Zeng and Grigg[13] The higher coefficients result in a higher pressure drop as expected.

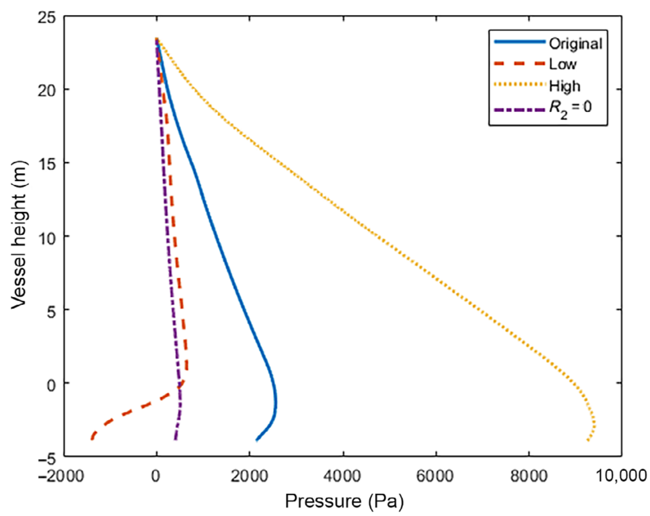

FIGURE 12 Pressure profile trough reactor for various values of R_1 and R_2.

6 | DISCUSSION AND CONCLUSIONS

The continuum model of the granular material wood chips captures the periodical behaviour of the formation and breakage of arches and also the periodicity of the corresponding hydraulic pressure variations, which is previously seen in when modelling smaller system, with limited amount of particles using DEM. The advantage of using the Eulerian continuum model approach is the ability to describe larger systems with billions of particles where heat and mass transport as well as chemical reactions can be included. The formation and collapse of the arch is present in all variations examined in this parameter sensitivity analysis, which suggests that it can be geometrical problem; however, the behaviour is more pronounced with certain choices of material constants, resulting in arch formation at higher values of chips volume fraction. In this work, the model presented is two-dimensional, and the geometry and boundary conditions are symmetrical. An introduction of an asymmetrical boundary condition or a disturbance would need a three-dimensional model to capture the effect. The two-dimensional model is stiffer due to one less degree of freedom, which could probably over-predict the formation of arches. A three-dimensional model would have instabilities in the tangential direction which could lead to less packing and hence breakage of structures before complete arch formation.

As mentioned in the introduction, the solid pressure is an important parameter for modelling of chips in pulping equipment; by varying the model constant P_{S0}, it is noted that the level of packing of the chips is significantly affected, which is in accordance with the findings of Hinterreiter et al.[16] where P_{S0} can be regarded as a lumped constant for moist content, shape, and aspect ratio. This is important since it affects the distribution of cooking liquid. Another aspect is the risk of the equipment malfunctioning; the stiffer chips will not pack to the same extent as a softer one, and an incorrect choice might under or overestimate the risk. The same effect can be noted when varying the wall friction coefficient; a higher wall friction coefficient, which corresponds to the wall carrying more of the load from the chips column, also results in a lower volume fraction in the bottom of the vessel. When comparing the results from the varying of the wall friction coefficient to the results from the solid pressure variation, the effect of the viscosity can be seen. Lowering P_{S0} results in lowering the load that the wall can carry, and also makes the chips more easily packed, or less viscous; the combined effect can be noted when comparing the left-most picture in Figures 6 and 8, where the volume fraction is higher in Figure 6. A lower viscosity results in an even higher volume fraction.

The same pattern can be seen when varying the constants of the permeability model; high coefficients result in a higher pressure drop since it corresponds to a less permeable chips column, and since it is less permeable, the liquid will not affect the distribution of the chips to the same extent and therefore also result in a less packed chips column. The corresponding lower pressure drop and higher volume fraction of chips can be seen with lower coefficients R_1 and R_2, as seen in Figures 11 and 12. Comparing the lower coefficients to R_1 as the base case and $R_2 = 0$, it can be seen that a similar pressure field and packing can be achieved with different set of constants. As $R_2 = 0$ corresponds to a situation where the inertial forces are negligible but calculating the Forchheimer number suggest that this is not the situation in the impregnation vessel further manifests that the coefficients should be carefully chosen and valid for the current situation.

It is important to avoid excessive packing of the pulping equipment since it aggravates the operation and could lead to uneven distribution of cooking chemicals. Therefore, when designing the equipment, the correct parameters for the intended bio material should be applied, and as shown by this parameter study, the solid pressure, wall friction, and permeability all affect the distribution of the volume fraction of wood chips. Since the solid pressure is affecting all properties of the chips column, it is perhaps the most important model parameter.

The values should not be taken in absolute terms but merely as an indication that the behaviour and outcome are affected by the model constant of choice; therefore, it is crucial to know the properties of the solid bio material used in the equipment to be able to predict the behaviour correctly. Pressure drop and distribution of liquid is dependent on the permeability of the column of chips, which in turn is dependent on the volume fraction of solids and can be viewed as a measure of the packing of the solid material, and the packing is in turn determined by the elasticity of the column made up of billions of solids, while the elasticity is modelled by the solid pressure.

AUTHOR CONTRIBUTIONS

Sofia Evysdotter: Writing – original draft; writing – review and editing; visualization. **Tomas Vikström:** Conceptualization; funding acquisition; methodology; project administration; supervision. **Anders Rasmuson:** Conceptualization; funding acquisition; project administration; supervision; methodology.

FUNDING INFORMATION

This article was funded by the Swedish Energy Agency-Project number 45123-1 and Valmet.

CONFLICT OF INTEREST STATEMENT

The authors declare no potential conflicts of interest.

PEER REVIEW

The peer review history for this article is available at https://www.webofscience.com/api/gateway/wos/peer-review/10.1002/cjce.25435.

DATA AVAILABILITY STATEMENT

The data that support the findings of this study are available from the corresponding author upon reasonable request.

ORCID

Sofia Evysdotter https://orcid.org/0009-0000-7750-0095

REFERENCES

[1] M. Kassberg, *Sulfatmassatillverkning*, 5th ed., Skogsindustrins Utbildning i Markaryd, Stockholm **1998**.
[2] E. J. Härkönen, *Tappi J.* **1987**, *70*, 122.
[3] F. A. Michelsen, B. A. Foss, *Applied Mathematical Modelling* **1996**, *20*, 523.
[4] P. A. Wisnewski, F. J. Doyle III, F. Kayihan, *AIChE J.* **1997**, *43*, 3175.
[5] S. Bhartiya, P. Dufour, F. J. Doyle III, *AIChE J.* **2003**, *49*, 411.
[6] Y. Fan, *PhD Thesis*, University of British Columbia (Vancouver, BC, Canada), **2005**.
[7] F. Kayihan, A. Bills, P. W. Hart, *AIChE J.* **2005**, *51*, 2489.
[8] K. Pougatch, M. Salcudean, I. Gartshore, *Applied Mathematical Modelling* **2006**, *30*, 209.
[9] R. Rantanen, *Modelling and Control of Cooking Degree in Conventional and Modified Continuous Pulping Processes*, Vol. 68, University of Oulu, Oulu, Finland **2006**.
[10] S. Laakso, *Modeling of Chip Bed Packing in a Continuous Kraft Cooking Digester*, Teknillinen korkeakoulu, Espoo **2008**.
[11] Q. F. Lee, *PhD Thesis*, University of British Columbia (Vancouver, BC, Canada), **2002**.
[12] M. Alaqqad, C. P. J. Bennington, D. M. Martinez, *Can. J. Chem. Eng.* **2012**, *90*, 1278.
[13] Z. Zeng, R. Grigg, *Transp. Porous Media* **2006**, *63*, 57.
[14] E. Ghane, N. R. Fausey, L. C. Brown, *Journal of Hydrology* **2014**, *519*, 3400.
[15] A. Drescher, A. J. Waters, C. A. Rhoades, *Powder Technol.* **1995**, *84*, 165.
[16] S. Hinterreiter, H. Hartmann, P. Turowski, *Biomass Convers. Biorefin.* **2012**, *2*, 109.
[17] J. Yoshida, *Adv. Powder Technol.* **1994**, *5*, 85.
[18] T. O. Kiwing, P.-Y. Lai, H. K. Pak, *Phys. Rev. Lett.* **2001**, *86*, 71.
[19] R. C. Hidalgo, C. Lozano, I. Zuriguel, A. Garcimartn, *Granular Matter* **2013**, *15*, 841.
[20] ANSYS, *Ansys CFX-Solver Theory Guide*, ANSYS, Inc., Canonsburg, PA **2024**.
[21] R. G. de Kretser, D. V. Boger, P. J. Scales, *Rheol. Rev.* **2003**, 125.
[22] S. Mahajan, M. Tennenbaum, S. Pathak, D. Baxter, X. Fan, P. Padilla, C. Anderson, A. Fernandez-Nieves, M. P. Ciamarra, *Phys. Rev. Lett.* **2020**, *124*, 128002.

How to cite this article: S. Evysdotter, T. Vikström, A. Rasmuson, *Can. J. Chem. Eng.* **2025**, *103*(2), 868. https://doi.org/10.1002/cjce.25435